UiT The Arctic University of Norway

Faculty of Science and Technology

Department of Physics and Technology

Determining optical-flow for turbulent motions in the aurora borealis

Kim André Jakobsen

FYS-3931 Master's thesis in Space Physics, June 2020

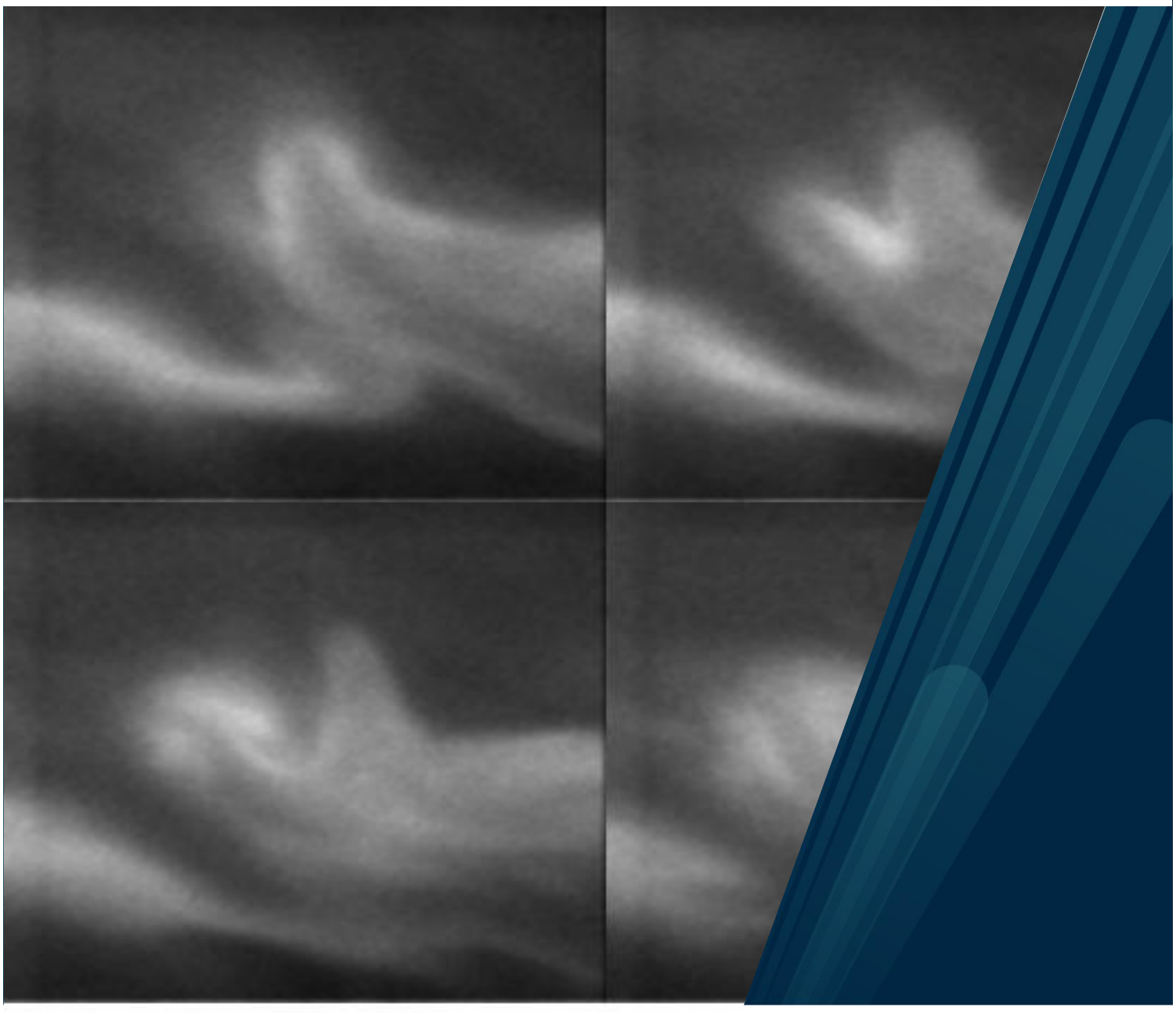

"Look deep into nature, and then you will understand everything better."

Albert Einstein

Abstract

In dynamic aurora there are structures that shows shear-flow and rotations. These flows have a locally varying vorticity-field, which can be observed in small scale aurora. Vorticity in plasma-flows have a direct relation to field-aligned currents. An effective method to determine these flows would be a great tool in research on magnetosphere-ionosphere coupling and auroral physics. With the current observations of aurora with high resolution and fps, it should be possible to determine these auroral motions with the use of optical-flow techniques. By using already existing methods, we show how well they work for turbulent motions in aurorae, and highlights advantages and disadvantages. A 20min recording with 32 fps have been studied, where a small image sequence containing several kinds of motions have been worked further on. By comparing differential techniques with phase-based techniques, we found that the differential techniques displayed better accuracy in turbulent flow. The phase-based provided good results for stable motions lasting a couple of frames, but there are still some adjustment thats should be done to optimize this technique for these kinds of motions.

The technique developed by Nagel provided the best results. This method maintained velocity gradients to a greater extent than other methods without the cost of significantly more noise. Although most methods provided reliable results, there are still work that must be done for a robust technique to use on aurorae in general.

Acknowledgement

I want to thank my supervisor, Professor Björn Gustavsson for the opportunity to write a thesis on such an interesting topic. Although the pandemic situation made communications slow, I'm grateful for the help and advice I've been given.

Contents

List of Figures

List of Abbreviations

ASK	Auroral Structure and Kinetics
FOV	Field Of View
FPS	Frames Per Second
LK	Lucas & Kanade
HS	Horn & Schunck
FJ	Fleet & Jepson

Chapter 1

Introduction

The northern light has been observed since ancient times. People have been curious of its source and fascinated by its existence for several thousands of years, which also accounts for a large part of the tourism industry at northern latitudes.

A clay tablet from more than 2500 years ago proves the aurora has been observed this early. The clay tablet contains numerous of celestial observation during one year (568/567 BC) [1]. The first known scientific and systematic observations were done by the swedish scientist Anders Celcius in the 18th century. Correlations between northern lights and the position of a magnetic needle were found and further science on this correlation were done. He was the first to suggest the connection between changes in the magnetic field of the earth and the aurora borealis [2].

As we know through research today, the northern light formation occurs through the following steps:

- Charged particles in the solar wind moves toward the earth
- These particles are trapped in the geomagnetic field-lines, where they accelerate along
- At northern latitudes, the field lines are close to vertical, hence the particles accelerate towards the polar atmosphere
- As the particles gets close to earth, the atmosphere gets thicker and the probability of collisions gets higher
- Most collisions happens on altitudes of $\sim$ 100km, where collisions with different kinds of molecules excites photons of their respective wavelengths

As technology has advanced in the last decades, it is now possible to record the northern lights with high resolution and *fps*. In this thesis a 20min recording has been analyzed with optical-flow techniques, to determine the turbulent motions to connect it to field aligned currents.

Several techniques to determine the optical-flow have been reviewed and applied to scenes of northern lights. The goal is to find a robust method to determine the optical flow from northern lights, which is a step towards being able to determine the field aligned currents in this area.

1.1 Report overview

The first part of this report is an introduction to the field of aurora borealis, which also includes a historical aspect. A description of the data and softwares follows in this introduction part. The next part explains the purpose and motivations for this work. Further, the theory of a couple of optical flow methods are presented with a physical description and the mathematical formulation to achieve the expected results. After the theories describing the methods, follows the experimental results. The last part contains discussion and conclusions, where different methods are compared. Advantages and disadvantages are discussed, ideas for future work with an ending conclusion for this thesis.

1.2 Data and software

The data used in this thesis was recorded by the ASK instruments which provides high resolution optical measurements. With FOV of 3.1°, the spatial size at $\sim$ 100km altitude is approximately 5km x 5km [6]. All experimental results of optical-flow velocity are given in unit [pixels/frame]. Given image size of 256 x 256, and fps: 32Hz, this unit can be transformed to [km/sec] by multiply the resulting speed with a factor of 0.625 as calculated in equation 1.1.

$$\frac{256pix}{5km} = 51.2pix/km$$

$$32frames/sec$$

$$\frac{pixels}{frame} = \frac{\frac{1}{51.2}km}{\frac{1}{32}sec} = 0.625km/sec \tag{1.1}$$

All experiments and simulations were done using MatLab with some downloaded program codes, and some written for this thesis. The program codes can be found in the appendix.

In later parts of this report, the Fourier-transform of the time evolution is processed. Nyquist sampling theorem states that $B < \frac{f_s}{2}$, hence the highest frequency should not be more than 16Hz, where B is the bandwidth and f_s is the sampling frequency (fps = 32Hz).

Chapter 2

Motivation

In small scale aurora there are apparent motion of the structures that show shear-flow or rotations. These kinds of aurora have a locally varying vorticity field that have a direct connection to field-aligned currents. An effective method to determine these optical flows and connect it to field aligned currents would be of great interest in research on magnetosphere-ionosphere coupling and auroral physics. The ASK instrument provides high resolution and fps image sequences. These should be detailed enough to get precise flow calculations with optical flow techniques.

As most of the existing optical-flow techniques have limited uses, they might not satisfy the nature of auroral motions. By testing the existing methods and modify for the purpose of aurora, a precise calculation of the flow can be determined. The goal is to find such a method to get a high resolution measurement of the currents in this part of the atmosphere. As these flows are directly connected to the field aligned currents, these measurements can help to understand the source of these current-fields which is partly unknown.

Chapter 3

Optical flow techniques

Optical flow is the apparent motion of objects in a visualized scene. A method which describes optical flow well in all possible cases has never been found, but there have been developed several techniques which works well for different cases. All of the techniques discussed in this chapter are well described in [3], which is the reference for these techniques.

3.1 Differential techniques

A fundamental method to determine the optical flow in an image sequence is through the assumption of constant intensity over time. This is described mathematically with the equation of conservation of intensity, which is a modified version of the conservation of mass-equation which relates image velocity with the time-change of intensity:

$$\frac{\partial I(\mathbf{x},t)}{\partial t} + \nabla I(\mathbf{x},t) \cdot \mathbf{u} = 0 \tag{3.1}$$

Here, I is the image intensity, $\mathbf{x}$ is the position vector (x, y), and $\mathbf{u}$ is the velocity vector $(u, v)^T$, and $\nabla I = \left(\frac{\partial I}{\partial x}, \frac{\partial I}{\partial y}\right)^T$. The equation indicates that an intensity change in one position is the result of motion in space.

(3.1) is an equation of two unknowns $\mathbf{u} = (u, v)$, thus the equation can not describe the image motion completely. A simple way to determine (u, v) can be done by finding the values for least-square-error for a specified region. This region must be large enough to not be significant affected by noise, but small enough to not contain multiple motions.

3.1.1 Lucas & Kanade

The LK-method is based on the minimizing of equation (3.1), with a weighted least-square fit [4]. This can be described mathematically by minimizing equa-

tion (3.2).

$$\sum_{x,y} W^2(\mathbf{x}) \left(\frac{\partial I(\mathbf{x},t)}{\partial t} + \nabla I(\mathbf{x},t) \cdot \mathbf{u} \right)^2 \tag{3.2}$$

where $W(\mathbf{x})$ is a window function which gives the most influence at the center of the window. Program codes for this equation are shown in the appendix.

3.1.2 Horn & Schunck

The method developed by Horn and Schunck uses the assumption of no velocity gradients in a specified region. This assumptions is not valid for a complete image sequence with turbulent flow, but can be used for small regions where we assume the flow is uniform. By minimizing equation (3.3) we get values for velocity (u, v) based on the HS-method.

$$\sum_{x,y} \left(\left(\frac{\partial I(\mathbf{x},t)}{\partial t} + \nabla I(\mathbf{x},t) \cdot \mathbf{u} \right)^2 + \lambda^2 \left(|\nabla u|^2 + |\nabla v|^2 \right) \right) \tag{3.3}$$

The equation was implemented by using Gauss-Seidel iterations [3] to find values for (u,v):

$$u^{k+1} = \bar{u}^k - \frac{I_x \left[I_x \bar{u}^k + I_y \bar{v}^k + I_t \right]}{\alpha^2 + I_x^2 + I_y^2} \tag{3.4}$$

$$v^{k+1} = \bar{v}^k - \frac{I_y \left[I_x \bar{u}^k + I_y \bar{v}^k + I_t \right]}{\alpha^2 + I_x^2 + I_y^2} \tag{3.5}$$

k is the iteration number, $(\bar{u}, \bar{v})$ are the average velocities in a chosen region and α is a constant which controls the influence of second-order derivative. Program codes for this implementation can be found in the appendix.

3.1.3 Nagel

In common with HS-method, the Nagel-method is also based on second-order derivatives. Nagel used an oriented smoothness constraint to not affect the steep intensity gradients.

$$\begin{aligned} &\sum_{x,y} \left(\frac{\partial I(\mathbf{x},t)}{\partial t} + \nabla I(\mathbf{x},t) \cdot \mathbf{u} \right)^2 \\ &\quad + \frac{\alpha^2}{|\nabla I|^2 + 2\delta} \left[(u_x I_y - u_y I_x)^2 + (v_x I_y - v_y I_x)^2 + \delta \left(u_x^2 + u_y^2 + v_x^2 + v_y^2 \right) \right] \end{aligned} \tag{3.6}$$

u_x, u_y, v_x, v_y are the velocity gradients in the respectively directions, and δ, α are constants chosen to make the required influence on the equation. Program codes can be found in the appendix.

3.2 Phase-based techniques

Another class of methods can be referred to as phase-based. By computing the Fourier transformation of an image sequence in time domain, we can determine the motions of objects by looking at the spatial evolution of the phases. Phases seems to be stable over time, which make these methods appear reliable for motion determination, and worth testing.

3.2.1 Fleet & Jepson

The method Fleet and Jepson developed, suggested that the image motion is related to the phase gradients. If we look at the different frequencies separately, we can define the phase as $\phi(\mathbf{x}, t)$. The Fourier transformation is computed in short time intervals to recover details of the motions. In Fleet and Jepson method, the velocity is defined by speed and direction as in (3.7) and (3.8).

$$s = -\frac{\phi_t(\mathbf{x}, t)}{||\nabla\phi(\mathbf{x}, t)||} \tag{3.7}$$

$$\mathbf{n} = \frac{\nabla\phi(\mathbf{x}, t)}{||\nabla\phi(\mathbf{x}, t)||} \tag{3.8}$$

This method might look straight forward, but since the phase of a signal is a value in the domain $[-\pi, \pi]$, values on the end points appear as sharp edges, when they in reality are close to each other. A solution for this problem is to use an *unwrapping*-function. This will make regions in the spatial distribution multiples of 2π, to get rid of the appearing phase-edges.

Chapter 4

Results

In this section, the experimental results are presented with figures and explaining text. All the techniques have been applied to a single event for comparison purpose. Figure 4.1 shows a small section containing four frames of the recorded motions. The two centered images were used in the experiment. These were chosen because they covers several types of motions. The first and last images were included to get a more complete context of the motions.

The result chapter is divided into sections where each section contains the results from one optical-flow technique.

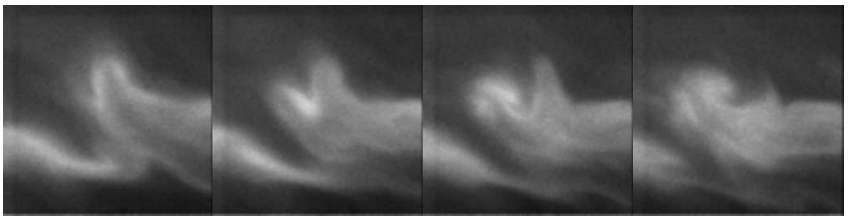

Figure 4.1: The evolution of aurora in a scene of four frames. The change between image 2-3 is analyzed with optical flow techniques. The images on each sides are included for overview purpose.

4.1 Lucas & Kanade

Since the LK-method uses a window function to calculate a weighted average velocity for a defined region, the images were not pre-filtered, since noise won't affect the results. The size of the window function should be large enough to contain motions over several pixels per frame, but small enough to not average

out important details of the motion. In this case the window function were chosen to be an all-ones matrix of size 16x16. The result is shown in figure 4.2. In a large scale basis, the result is very close to reality, but one must keep in mind that the window function averages out motion for the defined region, and therefore individual motions of small regions is lost in this process. This can also be seen in figure 4.3, where large regions have the same color. Transitions between different regions are smoothed out.

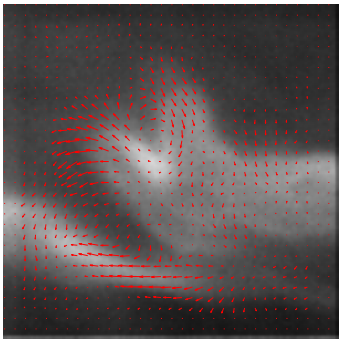

Figure 4.2: Velocity arrows using the LK-method with a window function size of 16x16.

By comparing the plots in figure 4.3 with the image sequence in figure 4.1, one can see that sharp blue or red areas describes the respective motions pretty well, however there is a lack of detailed motions.

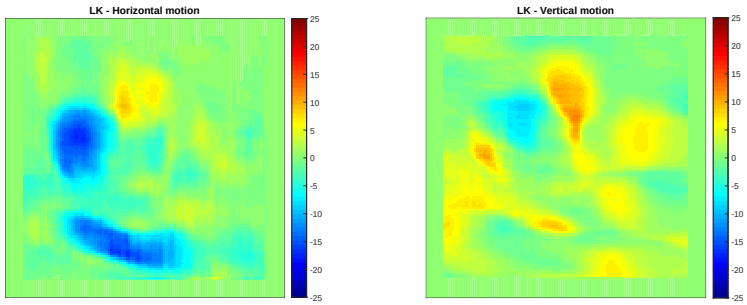

Figure 4.3: Spatial velocity distribution for the LK-method with a window function size of 16x16. Left and right image shows flow speed in horizontal and vertical direction respectively.

Another test was done with a window function of an all-ones matrix of size 8x8. This was done to get a more detailed plot of the motions. The edges are sharper, but more affected by noise because of the short averaging window. The velocity distributions are shown in figure 4.4, and for the case of windowing functions of 4x4 and 2x2 are shown in figure 4.5 and 4.6 respectively.

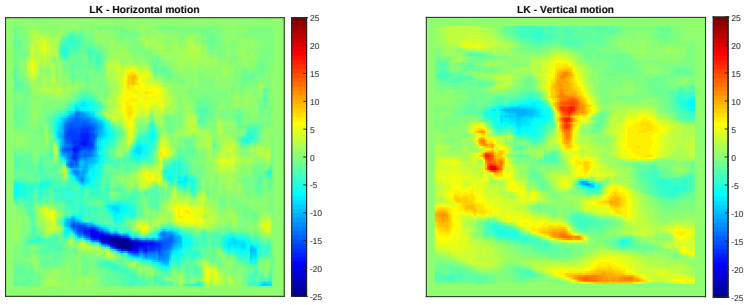

Figure 4.4: Spatial velocity distribution for the LK-method with a window function size of 8x8. Left and right image shows flow speed in horizontal and vertical direction respectively.

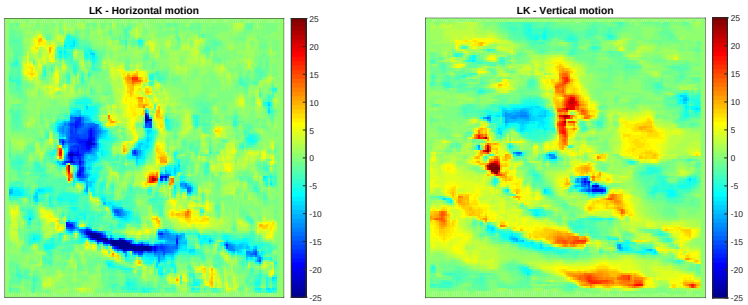

Figure 4.5: Spatial velocity distribution for the LK-method with a window function size of 4x4. Left and right image shows flow speed in horizontal and vertical direction respectively.

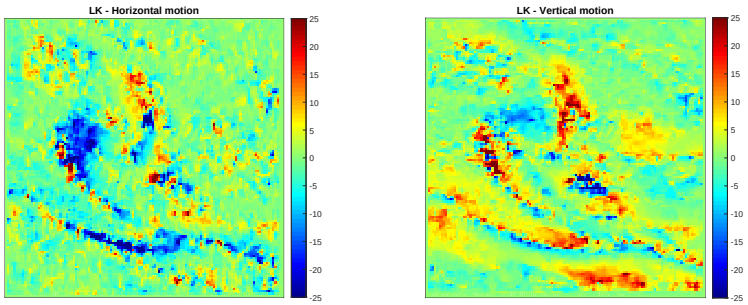

Figure 4.6: Spatial velocity distribution for the LK-method with a window function size of 2x2. Left and right image shows flow speed in horizontal and vertical direction respectively.

4.2 Horn & Schunck

The aurora is quite turbulent with different velocities. The assumption of no velocity gradients might therefore not hold. Since the flow is partially continuous, this assumption could still make good results if the influence from this term is not too great. The HS-method have been tested for the same two frames with

values $\alpha = 5$ and $\alpha = 15$. The number of iterations is 100 in both cases.

The first application of the HS-method was used with $\alpha = 5$ (figure 4.7 - 4.8). This gives a relatively low influence from the second order derivation term. The result is close to the LK-method with a medium sized window function.

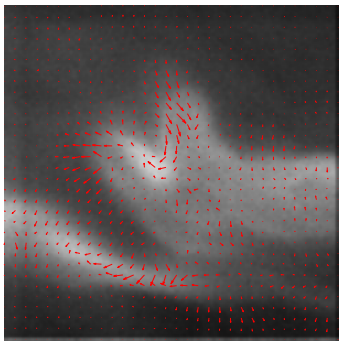

Figure 4.7: Velocity arrows using the HS-method with $\alpha = 5$.

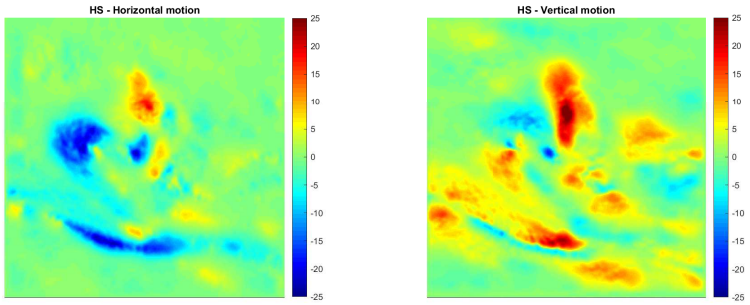

Figure 4.8: Spatial velocity distribution for the HS-method with $\alpha = 5$. Left and right image shows flow speed in horizontal and vertical direction respectively.

By using $\alpha = 15$ as in figure 4.9 - 4.10, areas are clearly more smoothed. That was suspected because of the nature of this method, which is minimizing the velocity gradients. As can be seen in the figure, different motions in a small area are averaged out, and only greater motion fields are left. This method works

in a way like a low-pass filter which compute the main optical- flow between two image scenes.

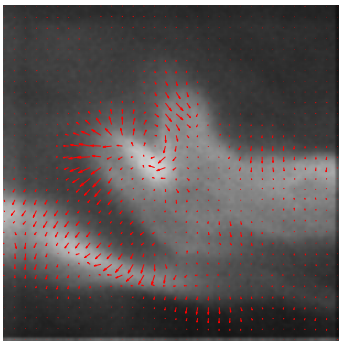

Figure 4.9: Velocity arrows using the HS-method with $\alpha = 15$.

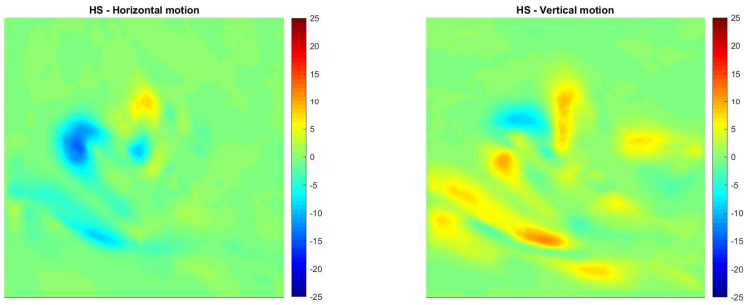

Figure 4.10: Spatial velocity distribution for the HS-method with $\alpha = 15$. Left and right image shows flow speed in horizontal and vertical direction respectively.

4.3 Nagel

As another "improvement" to the task to determine the optical-flow, the *oriented-smoothness* constraint suggested by Nagel was tested. The mathematical de-

scription of this method was shown in equation 3.6, by minimizing regarded to the velocity vector $\mathbf{u}$. In this application the constants were fixed to $\delta = 1$ and $\alpha = 0.5$, as suggested in [3]. Also other values were tested, but they led to inaccurate results or complications with the iterative calculations.

Figure 4.11 contains clear signs of turbulent flow in the center of the image. The result is not quite as good for collective motions at relatively large areas like the bottom left and central right part. However the bottom left area has a shear-like flow in the horizontal direction, and a collectively vertical drift downward.

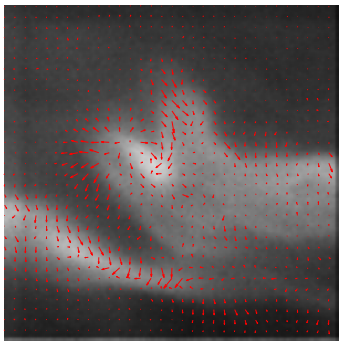

Figure 4.11: Velocity arrows using the Nagel-method with $\delta = 1$ and $\alpha = 0.5$.

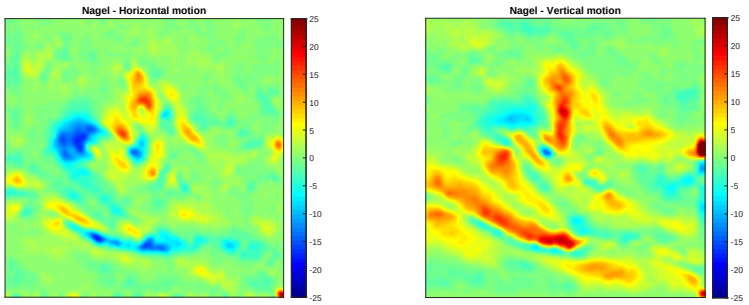

Figure 4.12: Spatial velocity distribution for the Nagel-method with $\delta = 1$ and $\alpha = 0.5$. Left and right image shows flow speed in horizontal and vertical direction respectively.

4.4 Fleet & Jepson

Aurora motions are quite turbulent in the time scale for the analyzed image sequence. Hence, a lot of motion changes occur in a small number of frames. If the interval that is Fourier-transformed gets too big, a lot of the phase information is lost in the process. The Fourier-interval must be short enough to not contain too much motion changes to keep the phase stable through time.

This technique was tested for two different settings, containing the same auroral event for comparison purpose. The first test was done for a time lapse of $\sim 0.75s$ (24 frames) with a Fourier-interval of 6 frames (4 overlapping). The second test with a time lapse of $\sim 0.375s$ (12 frames) with a fourier interval of 3 (1 overlapping).

The image sequence in figure 4.13 is the input data for this method. However the first test uses an additional six images before and six images after the event shown in this figure. The two images in center contains the motion we have been analyzed until now, and gonna continue to analyze with the help of surrounding images due to the nature of this method.

The Fourier-transformations were done in MatLab using the built in: *spectrogram*-function. This function takes the image sequence, preferred size of the Fourier-interval (number of frames) and overlapping frames as input.

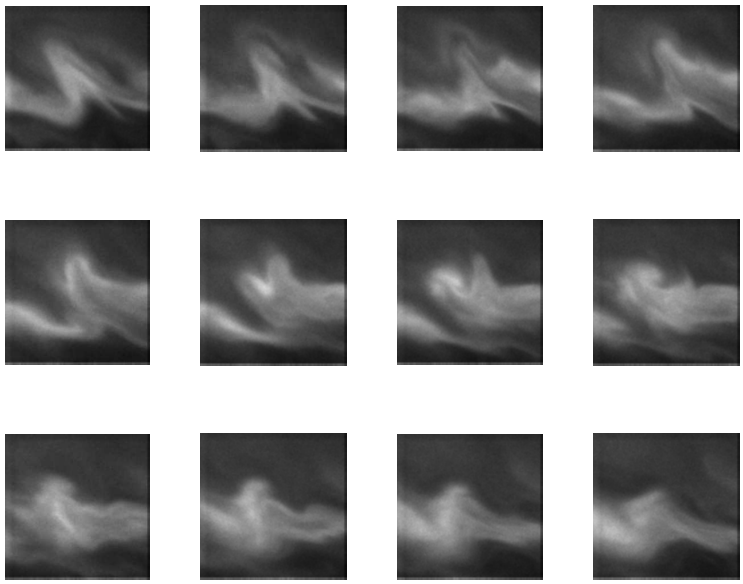

Figure 4.13: Sequence of 12 following images separated by $\sim$ 31ms. The two in center have been analyzed earlier.

4.4.1 Fleet & Jepson (6 frames, 4 overlapping)

To expect the phase is stable through an image sequence of 6 frames might be a somewhat crude assumption. As more information is used in the calculation, phases are more probable to change during time, partly because of occlusions. It was still tested for a measurement on how well it works.

This section contains the results of phase transformation around the three images in figure 4.14 defined as time: $t = 1, 2, 3$. Each image has a neighborhood of 5 images which were used to find the phases at the specified time, and the images are separated by $\sim 0.0625s$. These are the same images as number 5,7 and 9 in figure 4.13.

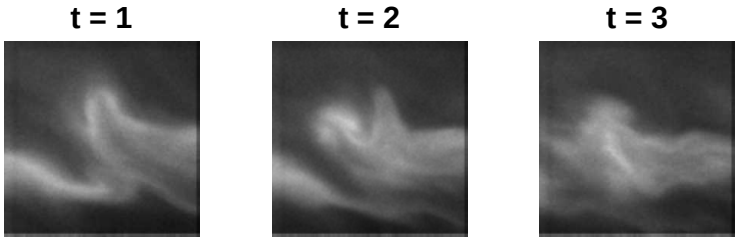

Figure 4.14: Image number 5, 7 and 9 in figure 4.13.

To get a complete overview of the phase variation, more than only one frequency should be analyzed. In figure 4.15 three different frequencies are plotted, two of them close to endpoints and one in the middle $(1, 8, 15\text{Hz})$.

There is a clear connection between the time steps of the images for all three frequencies. Therefore, it should be possible to calculate the optical flow from the derivatives which this method suggests. However, the phases are defined in the domain $[-\pi, \pi]$. This will in practice lead to unwanted phase hops in the transitions at endpoints, which again leads to unreal motions which should be taken care of.

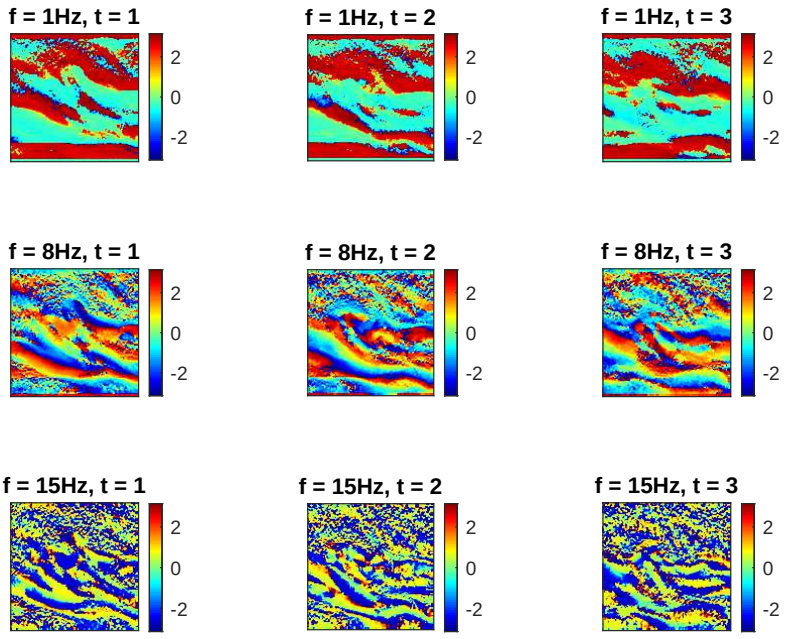

Figure 4.15: Spatial phase distribution at different frequencies and times with a fourier-interval of 6 images with 4 images overlapping. No unwrapping methods have been used.

Several so called unwrapping methods exists, which spreads the values out to avoid these unwanted phase hops. The method used in this thesis is based on the *minimum network flow*, which task is to limit the flow through the whole network of pixels. The algorithm used here was found on MathWorks File Exchanger: *Costantini phase unwrapping*, shared by *Bruno Luong*.

Figure 4.16 compared to 4.15 is in lack of the great phase hops which is the task we wanted to achieve. In addition, the clear edges which not is because of false phase hops have also been smoothed out. Despite this unwanted smoothing, there still seems to be some correlation of the phase distribution as function of time.

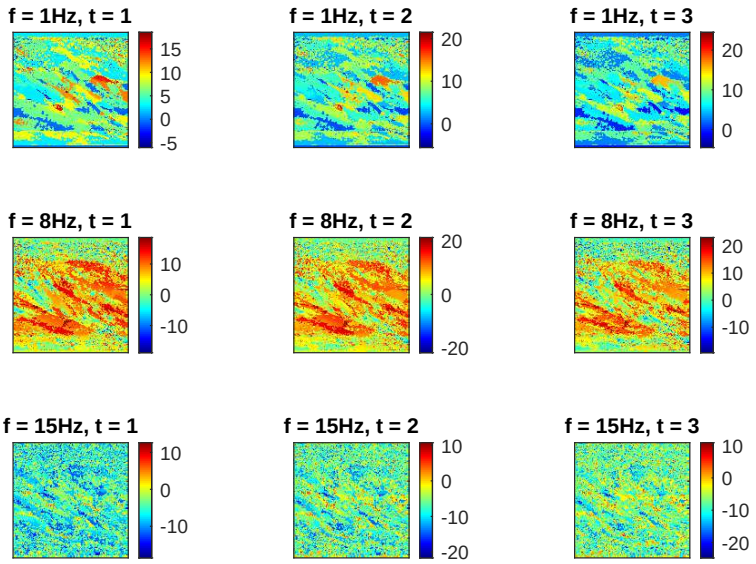

Figure 4.16: Spatial phase distribution at different frequencies and times with a fourier-interval of 6 images with 4 images overlapping. Phases are unwrapped beyond the interval $[-\pi, \pi]$.

The optical flow determined for $t = 1 \rightarrow 2$ and $t = 2 \rightarrow 3$ at $f = 8$Hz is shown in figure 4.17. The flow arrows indicates that there is a collective motion near the bottom left corner. This is consistent with other methods for the same auroral event. The vortex in center of the image is shown as more or less random distribution of motions. Because of the relatively great Fourier-interval, the phases in turbulent areas might change too fast for a continuously spatial phase motion.

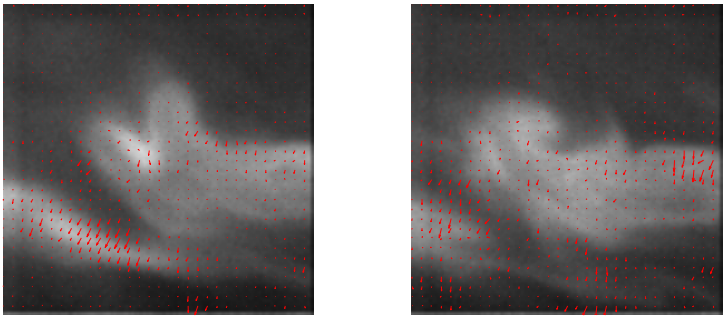

Figure 4.17: Velocity arrows using the FJ-method with fourier-interval of 6 images with 4 images overlapping. The Left and right image are the phase change $t = 1 \rightarrow 2$ and $t = 2 \rightarrow 3$ respectively in figure 4.16. Both at $f = 8$Hz.

4.4.2 Fleet & Jepson (3 frames, 1 overlapping)

With only 3 frames in each Fourier-transformation, the phase distributions should be more precisely describing the actual time. Again three moments in time are defined as $t = 1, 2, 3$ as in figure 4.18.

Figure 4.18: Image number 4, 6 and 8 in figure 4.13.

The same procedure as the last test was used to get the phase distribution in figure 4.19 with phases spread beyond the interval of $[-\pi, \pi]$.

The plots in this figure shows the spatial phase evolution is poorly dependent on frequency. That is because of the small number of frames in the transformation.

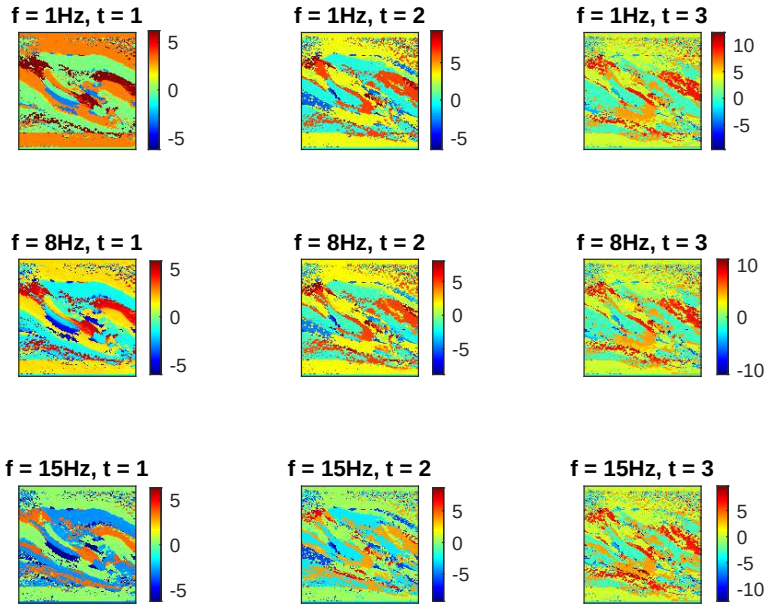

Figure 4.19: Spatial phase distribution at different frequencies and times with a fourier-interval of 3 images with 1 image overlapping. Phases are unwrapped beyond the interval $[-\pi, \pi]$.

Also in this test, the 8Hz spatial phase flow was used to determine the optical flow (presented in figure 4.20). The detailed turbulent motion is poorly represented in this plot. The collective motion of the whole event to the bottom left is also here dominating.

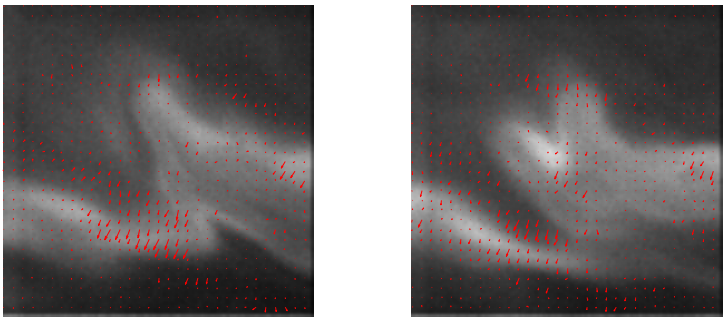

Figure 4.20: Velocity arrows using the FJ-method with fourier-interval of 3 images with 1 image overlapping. The Left and right image are the phase change $t = 1 \rightarrow 2$ and $t = 2 \rightarrow 3$ respectively in figure 4.19. Both at $f = 8$Hz.

Chapter 5

Discussion and Conclusion

A couple of different techniques have been used to determine the optical flow from an auroral event. The main focus of this thesis was to apply already known techniques for determining optical flow on auroral events. Because of the turbulent nature of aurora motions, the basic constraints used to track motion from an image sequence was not assumed to hold. By introducing new constraints which fits the nature of aurora motions, the results could get as close to reality as possible.

This chapter contains advantages and disadvantages with the different techniques, a detailed comparison, ideas for further work on this topic and finally: a conclusion.

5.1 Optical-flow techniques

Starting off with the LK-method [4], which defines the optical flow as the solution which gives the least deviation from intensity conservation in a chosen area (figure 4.2 - 4.6). When this area is large, areas of motion gets spatially smoothed. This might be an advantage if the goal is to get an overview on how the scene is moving as a whole, but at expense of motions at small scales. With small areas, the method led to precise results with a very small degree of spatial smoothing. The edges were sharp which clearly makes a border where the motions happens. In absence of the influence of neighboring pixels, noise related to the instruments, and occlusion because of the 2d representation of the 3d world is not taken care of.

Moving on to the HS-method [5], where a second order derivative is introduced (figure 4.7 - 4.10). The share-like-flow shown in the LK-method is also present in the results of the HS-method. With low influence of the second order derivative term, sharp velocity edges are present. As influence of the second-order derivative term is higher, the velocities are spatially smoothed close to the LK-method with large averaging areas.

The results from the Nagel-method are different from the two previous meth-

ods. The plots in figure 4.12 contains more velocity variations. There are parts with clear signs of share-flow and source/sink phenomena. In the previous two methods some of these were smoothed out. Due to the nature of aurora, these phenomena are clearly of existence because of compressibility and share-flow observations.

The last method which has a completely different procedure to implement, is the Fleet and Jepson-method. As this method requires a couple of frames for each fourier-transformation to calculate the phases, fast changes in motion could not be tracked. By using frame sequences of only 3 and 6 images, the phase motions were analyzed to map the velocities.

In both cases (figure 4.17 and 4.20), movement in one direction for a couple of frames can be observed. Areas with complicated motions as in the center of these plots are very affected by random motions, and should not be used for motion determination.

5.2 Further work

As it has been shown in this report, there are many methods to determine the optical flow. Only a few are applied here. Even though they gave good results in the bigger picture, the small scale motions are still inadequate.

Further work could be to set up new constraints that are more appropriate for the nature of aurora motions. A combination of different constraints with regulated influences could also make interesting results. Individual areas could be determined separately, and the final results could be combined in a coarse-to-fine manner as described in [7] and [8]. It should be possible to optimize an algorithm for a low cost of computation time.

The idea of handling the phase information should also be worked more on. There have been developed several unwrapping techniques, which should be tested, and find the technique that best suits this kind of motions.

5.3 Conclusion

In this work, optical flow techniques have been applied to an auroral event. An introduction to the physics of Aurorae and optical flow techniques which forms the basis for this work has also been give.

By determining the optical flow using different techniques, advantages and disadvantages have been shown. As the method developed by Fleet and Jepson treats the fourier transformed time variation, fast changing velocities have been smoothed out. Because of the phase stability, this method seems to be useful for linear motions through several frames. As the differential methods determined motions on a frame to frame basis, these methods gave a more exact solution of the optical flow. Unlike the HS- and LK-method, Nagel-method did not smooth along steep intensity gradients, which made edges more clear without allowing significantly more noise.

Although only a short number of frames were analyzed, these frames covers several kinds of motions in small scale aurora (vortices, linear and apparently compressible motions).

As a conclusion, the differential techniques provided the best detailed results, however the phase-based technique was only tested with a single unwrapping function. A more specified work on the phase-based techniques with several different unwrapping algorithms could lead to better results.

Appendix

Programming codes: Lucas & Kanade

The programming code is a modified version of the code on MathWorks File Exchanger: *Lucas-Kanade Tutorial Example 1*, shared by *Zhiyuan*.

```
function [u,v] = LKOpticalFlow(fr1, fr2, ww)
%% [u,v] = LKOpticialFlow(fr1, fr2, ww)
%
% Purpose: Calculates the optical flow between two frames based on the
%          Lucas & Kanade method.
%
% Inputs:
% - fr1 - 1st frame [Intensity 0-255], 2D - array.
% - fr2 - 2nd frame [Intensity 0-255], 2D - array.
% - ww - Windowing function [], n x n - array.
%
% Outputs:
% - u - Optical flow in horizontal direction [pixels/frame], 2D - array.
% - v - Optical flow in vertical direction [pixels/frame], 2D - array.

%% Resizing
im1t = fr1;
im1 = imresize(im1t, 0.5); % downsize to half

im2t = fr2;
im2 = imresize(im2t, 0.5); % downsize to half

%% Implementing Lucas Kanade Method
w = round(ww/2);

Ix_m = conv2(im1,[-1 1; -1 1], 'valid'); % partial on x
Iy_m = conv2(im1, [-1 -1; 1 1], 'valid'); % partial on y
It_m = conv2(im1, ones(2), 'valid') +...
    conv2(im2, -ones(2), 'valid'); % partial on t
```

```
u = zeros(size(im1));
v = zeros(size(im2));

for i = w+1:size(Ix_m,1)-w         % Calculates optical flow inside ww-window
    for j = w+1:size(Ix_m,2)-w
        Ix = Ix_m(i-w:i+w, j-w:j+w);
        Iy = Iy_m(i-w:i+w, j-w:j+w);
        It = It_m(i-w:i+w, j-w:j+w);

        Ix = Ix(:);
        Iy = Iy(:);
        b = -It(:);             % get B here

        A = [Ix Iy];            % get A here
        nu = pinv(A)*b;         % get velocity here

        u(i,j)=nu(1);
        v(i,j)=nu(2);
    end
end
end
```

Programming codes: Horn & Schunck

This is a modified version of the code on MathWorks File Exchanger: *Horn-Schunck Optical Flow Method*, shared by *Mohd Kharbat*.

```
function [u,v] = HS(im1, im2, alpha, ite)
%% [u,v] = HS(im1, im22, alpha, ite)
%
% Purpose: Calculates the optical flow between two frames based on the
%           Horn & Schunck method.
%
% Inputs:
%  - im1 - 1st frame [Intensity 0-255], 2D- array.
%  - im2 - 2nd frame [Intensity 0-255], 2D- array.
%  - alpha - Influence of the second order derivation term [], number.
%  - ite - Number of iterations [], number.
%
% Outputs:
%  - u - Optical flow in horizontal direction [pixels/frame], 2D- array.
%  - v - Optical flow in vertical direction [pixels/frame], 2D- array.

%%
% Set initial value for the flow vectors
```

```
u = zeros(size(im1));
v = zeros(size(im2));

% Estimate spatiotemporal derivatives
[fx, fy, ft] = computeDerivatives(im1, im2);

% Averaging kernel
kernel_1=[1/12 1/6 1/12;1/6 0 1/6;1/12 1/6 1/12];

% Iterations
for i=1:ite
    % Compute local averages of the flow vectors
    uAvg=conv2(u,kernel_1,'same');
    vAvg=conv2(v,kernel_1,'same');
    % Compute flow vectors constrained by its local average and the optical flow con
    u= uAvg - ( fx .* ( ( fx .* uAvg ) + ( fy .* vAvg ) + ft ) ) ./ ( alpha^2 + fx.^2
    v= vAvg - ( fy .* ( ( fx .* uAvg ) + ( fy .* vAvg ) + ft ) ) ./ ( alpha^2 + fx.^2
end

u(isnan(u))=0;
v(isnan(v))=0;
end



function [fx, fy, ft] = computeDerivatives(im1, im2)
%% [fx, fy, ft] = computeDerivatives(im1, im2)
%
% Purpose: Computing the derivatives fx, fy, ft.
%
% Inputs:
%  - im1 - 1st frame [Intensity 0-255], 2D - array.
%  - im2 - 2nd frame [Intensity 0-255], 2D - array.
%
% Outputs:
%  - fx - Array of gradients in x-direction [Intensity/pixel], 2D - array.
%  - fy - Array of gradients in y-direction [Intensity/pixel], 2D - array.
%  - fx - Array of time-derivatives [Intensity/frame], 2D - array.

fx = conv2(im1,0.25* [-1 1; -1 1],'same') +...
    conv2(im2, 0.25*[-1 1; -1 1],'same');
fy = conv2(im1, 0.25*[-1 -1; 1 1], 'same') +...
    conv2(im2, 0.25*[-1 -1; 1 1], 'same');
ft = conv2(im1, 0.25*ones(2),'same') + conv2(im2, -0.25*ones(2),'same');
end
```

Programming codes: Nagel

This is an iterative way to calculate the optical flow using the method developed by Nagel.

```
function [u,v] = Nagel(images, delta, alpha, ite)
%% [u,v] = Nagel(images, delta, alpha, ite)
%
% Purpose: Calculates the optical flow between two frames based on the
%          Nagel method.
%
% Inputs:
% - images - Array containing two frames [Intensity 0-255],
%            n x n x 2 - array.
% - delta - Delta value in the equation for optical flow [], number.
% - alpha - Alpha value in the equation for optical flow [], number.
%
% Outputs:
% - u - Optical flow in horizontal direction [pixels/frame], 2D - array.
% - v - Optical flow in vertical direction [pixels/frame], 2D - array.


[sy, sx, st] = size(images);     % Sizes of the input array.

kernel_1=[1/12 1/6 1/12;1/6 0 1/6;1/12 1/6 1/12]; % Weighted averaging.

%% Calculate derivatives
[dx, dy, dt] = computeDerivatives(images(:,:,1),images(:,:,2));
[dxx, dxy] = computeDerivatives(dx,1);
[dyx, dyy] = computeDerivatives(dy,1);

%% initial velocities
u = zeros(sy,sx,1);
v = zeros(sy,sx,1);

%% Calculate W and q
for j = 1:sx
    for i = 1:sy
        W(:,:,i,j) = (dx(i,j)^2+dy(i,j)^2+2*delta)^(-1)*[dy(i,j)^2+...
            delta -dx(i,j)*dy(i,j); -dx(i,j)*dy(i,j) dx(i,j)^2+delta];

        q(:,i,j) = 1/(dx(i,j)^2+dy(i,j)^2+2*delta)*[dx(i,j) dy(i,j)]*...
            ([dyy(i,j) -dxy(i,j); -dxy(i,j) dxx(i,j)]+...
            2*[dxx(i,j) dxy(i,j); dxy(i,j) dyy(i,j)]*W(:,:,i,j));
    end
end
```

```
%% Calculating velocity iterative

for it = 1:ite
        avg_u = conv2(u,kernel_1,'same');    % Averages and velocity -
        avg_v = conv2(v,kernel_1,'same');    % derivatives are calculated
                                             % again for every iterations.
        [dux, duy] = computeDerivatives(u,1);
        [dvx, dvy] = computeDerivatives(v,1);

        [duxx, duxy] = computeDerivatives(dux,1);
        [dvxx, dvxy] = computeDerivatives(dvx,1);

    for j = 1:sx
        for i = 1:sy
            zeta_u(i,j) = avg_u(i,j) - 2*dx(i,j)*dy(i,j)*duxy(i,j)-...
                reshape(q(:,i,j),1,2)*[dux(i,j);duy(i,j)];

            zeta_v(i,j) = avg_v(i,j) - 2*dx(i,j)*dy(i,j)*dvxy(i,j)-...
                reshape(q(:,i,j),1,2)*[dvx(i,j);dvy(i,j)];

            M = (dx(i,j)*zeta_u(i,j)+ dy(i,j)*zeta_v(i,j)+...
                dt(i,j))/(dx(i,j)^2+dy(i,j)^2+alpha^2);

            u(i,j) = zeta_u(i,j) - M*dx(i,j);
            v(i,j) = zeta_v(i,j) - M*dy(i,j);
        end
    end
end
```

Bibliography

[1] F. R. Stephenson, D. M. Willis, T. J. Hallinan (2004). *The earliest datable observation of the aurora borealis.* Astronomy & Geophysics, Volume 45, Issue 6, 6.15-6.17.

[2] Wikipedia 2020, Anders Celcius, viewed 10 April 2020, https://en.wikipedia.org/wiki/Anders_Celsius.

[3] J. L. Barron, D. J. Fleet, and S. S. Beauchemin (1994). *Performance of Optical Flow Techniques.* International journal of computer vision, 12(1), 43-77.

[4] B. Lucas, T. Kanade (1981). *An iterative image registration technique with an application to stereo vision.* Proc. DARPA IU Workshop, 121–130.

[5] B. K. P. Horn, B. G. Schunck (1981). *Determining optical flow.* AI 17, 185-204

[6] I. Sandahl (2009). *In the light of the aurora.* Network for Groundbased Optical Auroral Research in the Arctic Region.

[7] J. Y. Bouguet (2000). *Pyramidal implementation of the Lucas Kanade feature tracker.* Intel Corporation. Microprocessor Research Labs.

[8] X. Chen, P. Zillé, L. Shao, T. Corpetti (2015). *Optical flow for incompressible turbulence motion estimation.* Experiments in Fluids 56, Article number: 8.